

# Modelling the Propagation of a Weak Fast-Mode MHD Shock Wave near a 2D Magnetic Null Point Using Nonlinear Geometrical Acoustics

A.N. Afanasyev · A.M. Uralov

© Springer ●●●

**Abstract** We present the results of analytical modelling of fast-mode magnetohydrodynamic wave propagation near a 2D magnetic null point. We consider both a linear wave and a weak shock and analyse their behaviour in cold and warm plasmas. We apply the nonlinear geometrical acoustics method based on the Wentzel–Kramers–Brillouin approximation. We calculate the wave amplitude, using the ray approximation and the laws of solitary shock wave damping. We find that a complex caustic is formed around the null point. Plasma heating is distributed in space and occurs at a caustic as well as near the null point due to substantial nonlinear damping of the shock wave. The shock wave passes through the null point even in a cold plasma. The complex shape of the wave front can be explained by the caustic pattern.

**Keywords:** Magnetohydrodynamics; Waves, Propagation; Waves, Shock; Heating, Coronal

## 1. Introduction

Various eruptive processes in the solar atmosphere as well as convective motions beneath the photosphere generate magnetohydrodynamic (MHD) waves. Propagation of waves in an inhomogeneous plasma can result in wave energy dissipation, which is known to contribute into the general energy balance of the solar corona. Behaviour of MHD waves is governed by the topology of magnetic field and gradients of MHD quantities. Singularities of the magnetic field topology are null points, at which the magnetic field magnitude is equal to zero.

Dissipation of the wave energy is believed to occur most efficiently near magnetic null points. In the solar corona, where the plasma beta is much less than unity, a fast-mode MHD wave is subject to significant deceleration at nulls, which therefore are the regions of the accumulation of the wave energy. The amplitude of the wave and gradients of all MHD quantities increase considerably due to the Alfvén speed decrease as well as the wave front convergence in the vicinity

---

Institute of Solar-Terrestrial Physics SB RAS,  
P.O. Box 291, Lermontov St. 126A, Irkutsk 664033, Russia  
email: afa@iszf.irk.ru email: uralov@iszf.irk.ru

of the null point, where the wave becomes nonlinear. The wave profile steepens and the initially linear wave transforms into a shock. Another important effect of the increase of the gradients is the appearance of steep spikes of the electric current density in the vicinity of the null point, as it was demonstrated by Foullon *et al.* (2005) and modelled numerically by McLaughlin and Hood (2004) and Nakariakov *et al.* (2006). These circumstances result in rapid conversion of the wave energy into heat.

Topological properties of magnetic null points have been studied well (see, *e.g.*, the review by Longcope, 2005) and the behaviour of waves in the vicinity of a null point has been investigated by many authors (see the review by McLaughlin, Hood, and De Moortel, 2011). McLaughlin and Hood (2004) consider the incidence of a linear fast-mode wave on a 2D null point both numerically and analytically using the Wentzel–Kramers–Brillouin (WKB) approximation. The authors neglect the plasma pressure against magnetic pressure and assign the sound speed to be zero. Their analysis shows that ray paths along which the wave travels get curved towards the null point due to refraction. The wave envelops the null point and its energy is converted to heat. Then McLaughlin and Hood (2006a) consider the wave incidence on a 2D null point formed by two magnetic dipoles. In this case, only a portion of the wave and its energy are captured by the null point. The rest propagates away.

The assumption of zero sound speed is a significant restriction for the problem of interest. The solar coronal plasma has a temperature of about  $1.5 \times 10^6$  K, which gives a sound speed of about  $180 \text{ km s}^{-1}$ . There is an area around the null point, in which the sound speed  $c$  is greater than the Alfvén speed  $V_A$ . This considerably affects wave propagation. The wave is able to pass through the null point in this case. A numerical modelling and analytical analysis of this problem is carried out, in the linear approximation, by McLaughlin and Hood (2006b). In their numerical study, they also find conversion of the wave modes when the wave crosses the  $V_A = c$  layer.

Further, McLaughlin, Ferguson, and Hood (2008) consider the wave propagation near a 3D magnetic null point under the assumption of cold plasma, using the WKB approach. This investigation confirms capturing the wave by the null point as well as plasma heating at that place. We note that in the analytical studies mentioned, the authors model only the wave front propagation and do not examine the wave amplitude evolution.

The propagation of a nonlinear wave near a magnetic null point is investigated by McLaughlin *et al.* (2009) for the magnetic reconnection problem. Their numerical modelling shows a complex pattern including the formation of a current sheet as well as the generation of secondary shock waves. Using a similar numerical approach, Gruszecki *et al.* (2011) study the nonlinear wave propagation to understand the triggering of the sympathetic solar flares.

The aim of this paper is to analyse analytically nonlinear effects of the weak fast-mode MHD shock wave propagation near a magnetic null point and calculate the wave amplitude evolution for the coronal heating problem. We do not study mode conversion as well as the transformation of the null point into a current sheet by the shock wave, since the ray method is not able to take this into account. The paper has the following outline. We consider the linear wave case

in Section 2, then the case of a shock wave in Section 3 and discuss the results obtained. Section 4 contains concluding remarks. In the Appendices we give bulky mathematical details of our investigation.

## 2. Linear wave

In this study we explore a two-dimensional magnetic null point, which is located at the point of origin and specified in Cartesian coordinates  $(x, y, z)$  as  $\mathbf{B} = (x, 0, -z)$  (see, *e.g.*, Parnell *et al.*, 1996). In this model, the magnetic field magnitude grows linearly with the distance from the null point. The plasma density  $\rho$  and temperature  $T$  are assumed to be constant, so the sound speed  $c = \sqrt{2\gamma R_{gas}T/\tilde{m}M_H}$  is also constant and the Alfvén speed  $V_A = B/\sqrt{4\pi\rho}$  distribution is governed only by that of the magnetic field. Here  $M_H$  is the molar mass of hydrogen,  $\tilde{m}$  the average atomic weight of an ion,  $\gamma$  the adiabatic index, and  $R_{gas}$  the gas constant. The Alfvén speed vanishes completely at the null point and grows to infinity away from it.

### 2.1. Cold plasma

At first we consider the case of a cold plasma, with the sound speed  $c$  being zero overall. Let a linear plane fast-mode MHD wave propagate towards the magnetic null point. To calculate its propagation, we apply the geometrical acoustics method (WKB approach). In this method, a solution is found in the form of  $A(\mathbf{r}, t)e^{i\Psi(\mathbf{r}, t)}$  where  $A(\mathbf{r}, t)$  is the wave amplitude, and  $\Psi(\mathbf{r}, t)$  is the eikonal, depending on both coordinates  $\mathbf{r} = (x, z)$  and time  $t$ . By substituting this representation for wave perturbations into the set of linearised equations of ideal magnetohydrodynamics, one can obtain a Hamilton–Jacobi partial differential equation for the eikonal of fast-mode MHD waves (see, *e.g.*, Uralova and Uralov, 1994):

$$\frac{\partial\Psi}{\partial t} + a|\text{grad}\Psi| = 0,$$

where  $a = 1/2\left(\sqrt{c^2 + V_A^2} + 2cV_A \cos\alpha + \sqrt{c^2 + V_A^2} - 2cV_A \cos\alpha\right)$  is the fast-mode velocity in plasma,  $\alpha$  the angle between the direction of the wave propagation and the magnetic field vector. Solving the equation with the method of characteristics gives the set of ray equations, which are a set of ordinary differential equations. In Appendix A we provide this set of equations (see Equations (5)). McLaughlin and Hood (2004) succeeded in finding an exact analytical solution of the set for the magnetic field model under consideration:

$$x = e^{-\frac{z_0}{r_0}t} \left( x_0 \cos \frac{x_0}{r_0}t + z_0 \sin \frac{x_0}{r_0}t \right), \quad z = e^{-\frac{z_0}{r_0}t} \left( z_0 \cos \frac{x_0}{r_0}t - x_0 \sin \frac{x_0}{r_0}t \right), \quad (1)$$

where  $r_0 = \sqrt{x_0^2 + z_0^2}$ , and  $x_0$  and  $z_0$  are the initial values of a ray path.

The null point attracts the wave, so all the ray paths tend to the origin where the null point is located. Figure 1 shows the ray pattern. In both the figures and

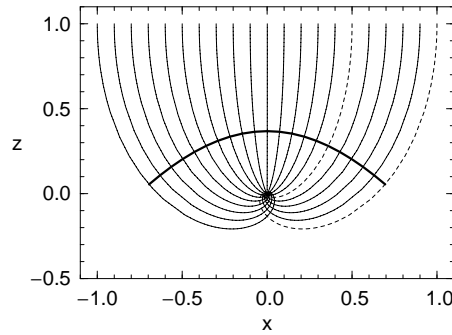


**Figure 1.** The propagation of a linear wave near a null point in a cold plasma. The thin lines represent the rays and the thick one marks the wave front at moment  $t = 1$ . At the initial moment, the plane wave front was located at  $z = 1$  and  $-1 \leq x \leq 1$ . The axes are shown in the normalised units.

calculations throughout the paper, we use normalised units. The normalising values are the characteristic spatial scale of the problem, and the magnetic field strength and the Alfvén speed at the distance of the characteristic spatial scale from the null point. The normalising time value is then set as the ratio of the characteristic spatial scale to the characteristic Alfvén speed.

However, it is essential not only to find the wave geometry, but also to calculate the wave intensity. Geometrical acoustics allows the wave amplitude variation to be calculated.

In linear geometrical acoustics, the energy flux of a disturbance travelling at group velocity  $\mathbf{q}$  in a stationary medium is directed along the rays, and its magnitude is conserved within a ray tube (Blokhintsev, 1981),  $\text{div}(\Delta\varepsilon\mathbf{q}) = 0$ , where  $\Delta\varepsilon = \rho(u^2 + v^2)$  is the average density of the disturbance energy,  $\rho$  the undisturbed plasma density, and  $u, v$  the plasma velocity components along the normal  $\mathbf{k}$  to the wave front and across it, respectively. Taking into account the relation between the plasma velocity components (Kulikovsky and Lyubimov, 2005),  $\mu = v/u = (1 - c^2/a^2) \cot \alpha$ , it is possible to relate the variation of the wave amplitude to the cross section  $dS$  of the ray tube formed by a bundle of rays:

$$dSq\rho u^2(1 + \mu^2) = \text{const}. \quad (2)$$

We calculate the cross section, using the Jacobian of the transformation from Cartesian coordinates to ray ones (Kravtsov and Orlov, 1990). The volume element  $dW$  of the ray tube is expressed in terms of the ray coordinates  $(\eta, t)$  as

$$dW = dx dz = D(t) d\eta dt, \quad D(t) = \begin{vmatrix} \partial x/\partial\eta & \partial x/\partial t \\ \partial z/\partial\eta & \partial z/\partial t \end{vmatrix},$$

where  $D(t)$  is the Jacobian. Then for the cross section of the ray tube,  $dS$ , we have

$$dS = \frac{dW}{d\sigma} = \frac{D(t)}{q} d\eta,$$

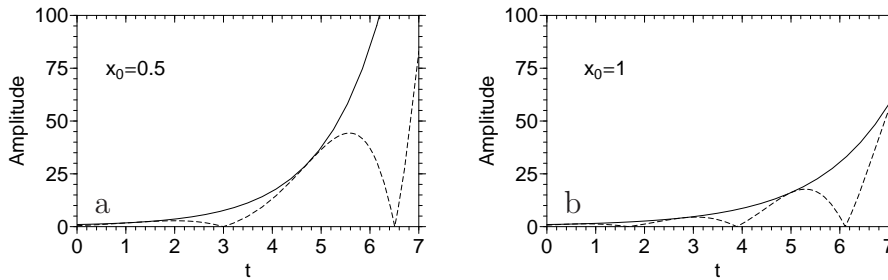


**Figure 2.** Evolution of the linear wave amplitude along the rays with  $x_0 = 0.5$  (a) and  $x_0 = 1$  (b) (marked as the dashed lines in Figure 1) in the cold plasma case. The dashed lines represent the plasma velocity component  $u$  along the normal to the wave front and the solid ones show the magnitude of the plasma velocity. The horizontal axes are shown in the normalised time units, the vertical axes are shown in the units of the initial amplitude.

where  $\sigma$  is the ray length. Let the ray coordinate  $\eta$  be the initial value  $x_0$ . Using Equations (1) and (2) we obtain the expressions for the wave amplitude  $A$  along the ray with the initial values  $x_0$  and  $z_0$  ( $A_0$  is the initial amplitude):

$$A(t) / A_0 = \left| \frac{x_0 \cos 2 \frac{x_0}{r_0} t + z_0 \sin 2 \frac{x_0}{r_0} t}{x_0} \right| \sqrt{\frac{r_0}{z_0 t + r_0}} e^{\frac{z_0}{r_0} t}, \quad (3)$$

if we assume the wave amplitude  $A$  to be the component  $u$  of the plasma velocity vector along the normal to the wave front, or

$$A(t) / A_0 = \sqrt{\frac{r_0}{z_0 t + r_0}} e^{\frac{z_0}{r_0} t}, \quad (4)$$

if we assume  $A$  to be the magnitude of the plasma velocity vector,  $A = \sqrt{u^2 + v^2}$ .

Figure 2 shows time evolution of the wave amplitude along two different rays. The amplitude plots in the paper are shown in the units of the initial amplitude. The plasma velocity component  $u$  oscillates and drops to zero from time to time, while the magnitude of the plasma velocity grows exponentially. Such behaviour of the component  $u$  is due to changing the direction of the wave propagation. The wave front element travels around the null point and sometimes the wave front normal  $\mathbf{k}$  becomes collinear to the magnetic field  $\mathbf{B}$ , *i.e.*  $\alpha = 0$  or  $\pi$ . At these points, the component  $u$  disappears but the component  $v$  becomes equal to the magnitude of the plasma velocity vector at that moment. There is also the opposite case: when the  $\alpha = \pm \pi/2$  the component  $v$  drops to zero. So the solid line marking the magnitude of the plasma velocity is an envelope line. Note that in Figure 2 we plot a relative variation of the amplitude and adjust the magnitude of the plasma velocity vector to be unity at the initial moment. It means that for the component  $u$  we actually use Equation (3) divided by  $r_0/|x_0|$ .

## 2.2. Warm plasma

Now we consider the case of a warm plasma with non-zero sound speed. Let points where the Alfvén speed is equal to the sound speed be named the  $V_A = c$

layer (see, *e.g.*, McLaughlin and Hood, 2006b). In the problem of interest, the case of a warm plasma corresponds to the situation when the wave propagates near the  $V_A = c$  layer, while in the case of a cold plasma the wave propagation is considered far from it. The ray equations become more complex and we have to integrate them numerically. To calculate the Jacobian and find the wave amplitude, we use a method based on numerical integration of the so-called adjoint set of equations. Solving the adjoint set allows the quantities  $\partial x/\partial \eta$  and  $\partial z/\partial \eta$  to be calculated. For more details, we refer the reader to the paper by Afanasyev and Uralov (2011). Appendix A contains the set of ray equations (see Equations (5)) as well as the adjoint set (see Equations (6)), which we solve to model the wave propagation.

Like McLaughlin and Hood (2006b) we find that the wave passes through the null point. Figure 3 shows the wave propagation in this case. We study behaviour of the wave front, which was located at  $z = 1$  and  $-2 \leq x \leq 2$  at the initial moment, however we plot the rays outgoing from a central part of the wave front for clearing the ray pattern. Unlike the cold plasma case, ray paths begin to intersect near the top boundary of the  $V_A = c$  layer. This results in the considerable distortion of the wave front as well as the subsequent formation of a caustic.

By definition, a caustic is an envelope of a family of rays, *i.e.* rays approach each other at points of the caustic (Kravtsov and Orlov, 1990), and therefore a caustic can be identified in the ray pattern as a ray crowding. The Jacobian and the ray-tube cross sections drop to zero at the caustic points and the wave amplitude grows indefinitely. Figure 4 shows evolution of the wave amplitude along two rays outlined by red in Figure 3. Marking points of the ray paths where the amplitude tends to infinity for the first time (since this can occur twice along some rays during the calculation time in our modelling) we can obtain the caustic line. The bottom panel in Figure 3 shows the inner part of the caustic, associated with a central part of the wave. The rest of the caustic encompasses the null point, bending away from it. The outer parts of the caustic form if the initial front is rather extensive. Besides, if the calculation time is also rather long it is possible to identify secondary (repeated) caustics. For instance, one of them can be seen in the top panel of Figure 3 as a cusp at the lower part of the plot. Note that in the linear cold plasma case there are no caustics in the neighbourhood of the null point.

The singular behaviour of the wave amplitude indicates that the ray approximation does not work at the caustic. Indeed, more accurate considerations show that the amplitude grows but it always remains finite (Kravtsov and Orlov, 1990). Nevertheless, caustics give important information on the amplitude distribution along the wave front. At every moment, the wave amplitude increases significantly at a few points (the caustic does not “fire up” simultaneously throughout its extent). Caustics in the ray pattern represent the places of the most efficient plasma heating associated with the wave. The energy of the wave accumulates in the neighbourhood of the null point, but this accumulation is distributed in space, unlike the cold plasma case. Our calculations show that the size of the  $V_A = c$  layer may be chosen as the characteristic spatial scale of the heated region around the null point.

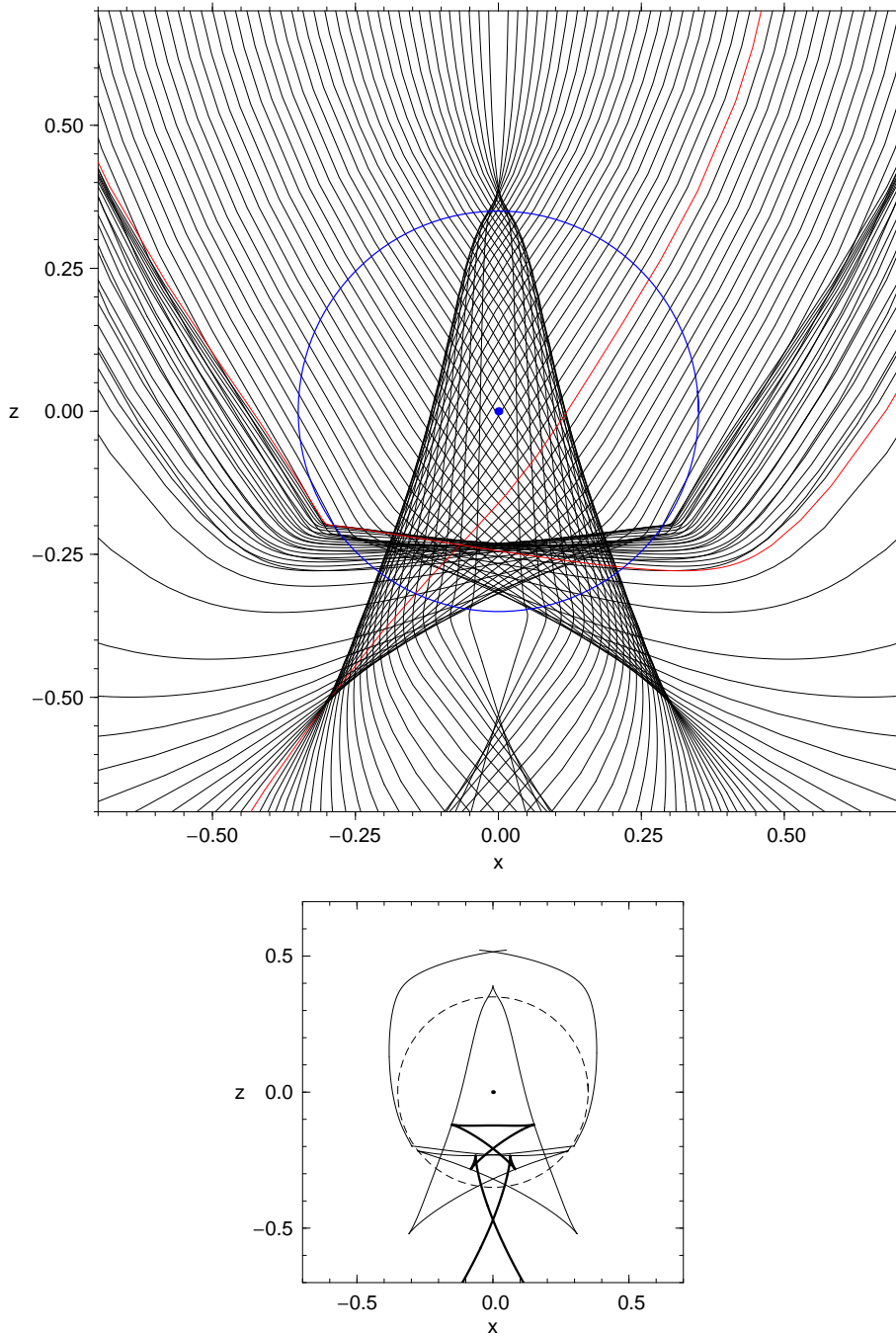


**Figure 3.** The propagation of a linear wave near a null point in a warm plasma: the ray pattern (top), and the wave front and the caustic (bottom). In the top panel, blue denotes the location of the  $V_A = c$  layer and the null point, black and red – the rays. In the bottom panel, the solid lines denote the wave front at moment  $t = 2.4$  (thick) and the caustic (thin), and the dashed line denotes the  $V_A = c$  layer. At the initial moment, the plane wave front was located at  $z_0 = 1$  and  $-2 \leq x \leq 2$ . The axes are shown in the normalised units.



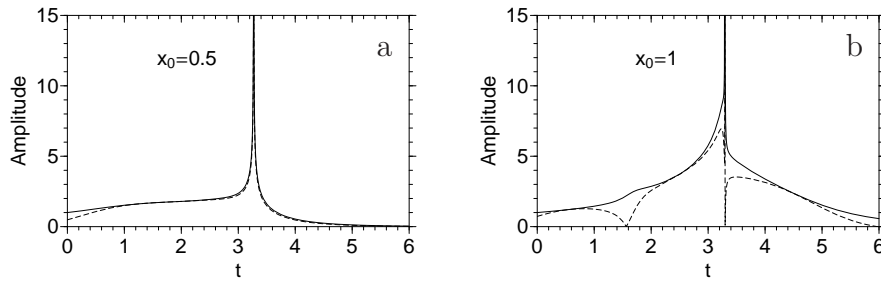


**Figure 4.** Evolution of the linear wave amplitude along the rays with  $x_0 = 0.5$  (a) and  $x_0 = 1$  (b) (red lines in Figure 3) in the warm plasma case. The dashed lines represent the plasma velocity component  $u$  along the normal to the wave front and the solid ones show the magnitude of the plasma velocity. The horizontal axes are shown in the normalised time units, the vertical axes are shown in the units of the initial amplitude.

Analysing the caustic pattern we can also readily explain the complicated surface of the wave front mentioned in McLaughlin and Hood (2006b). A break of the wave front occurs at the caustic (see Figure 3), so “small triangular shapes” of the wave front arise at the caustic cusps. Vertices of these triangles travel along the caustic lines as the wave front propagates.

### 3. Shock wave

As seen in Section 2.1, the wave amplitude grows exponentially as the wave approaches the null point. This results in the nonlinear steepening of the wave front and therefore a shock wave formation. So we should take into account nonlinear properties of shock waves and investigate how they affect the wave propagation.

Firstly, a nonlinear plane disturbance in an ideal homogeneous medium propagates at speed that exceeds the fast-mode velocity and depends on the disturbance amplitude. In a nonlinear acoustics approximation, a fast-mode wave element with plasma velocity component  $u$  normal to the front moves at a speed of  $a + \kappa u$ , where  $\kappa = (1/a)(d(\rho a)/d\rho)$  is the numerical coefficient depending both on the plasma beta and the angle  $\alpha$  between the wave front normal and the magnetic field (see Appendix A). The fact that each element of the wave travels at its own speed causes the wave profile deformation and the appearance of a shock wave. In turn, a weak shock moves at a speed of  $a + \kappa U_{sh}/2$ , where  $U_{sh}$  is the jump of the plasma velocity component  $u$  in the shock.

Secondly, the nonlinear wave amplitude undergoes additional damping associated with the energy dissipation in the discontinuity. On the one hand, the shock wave amplitude increases due to the convergence of rays as well as the Alfvén speed decrease. On the other hand, the amplitude decreases due to the nonlinear damping.

The above-mentioned basic properties of shock waves are taken into account in the method of nonlinear geometrical acoustics. It allows one to calculate the propagation of disturbances with small but finite amplitudes (*i.e.* weak shock



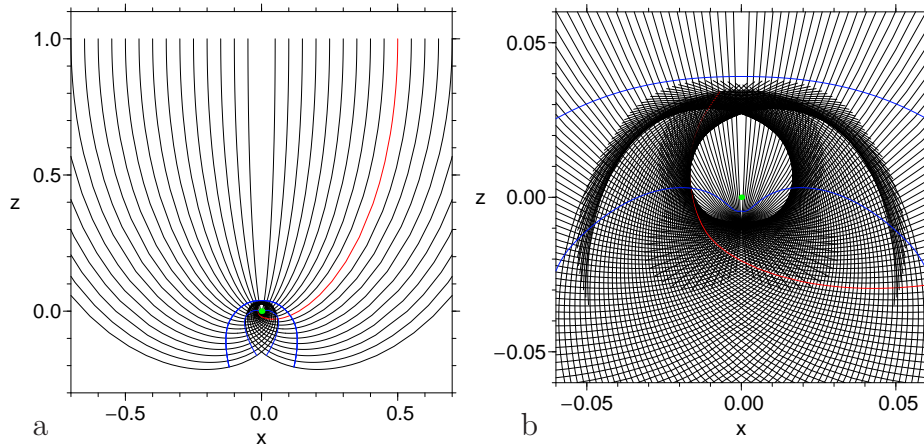


**Figure 5.** The propagation of a shock wave near a null point in a cold plasma. Blue colour denotes the positions of the wave front at moments  $t = 2.5$  and  $t = 3.0$ , green – the null point, black and red – the rays. At the initial moment, the plane wave front was located at  $z_0 = 1$  and  $-1 \leq x \leq 1$ . Panel b shows a zoom on the null point vicinity. The axes are shown in the normalised units.

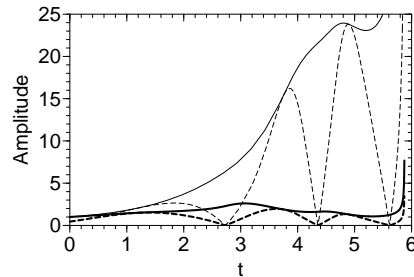


**Figure 6.** Evolution of the shock wave amplitude along the ray with  $x_0 = 0.5$  in the cold plasma case. The thick lines correspond to the amplitude of the shock wave and the thin ones correspond to the amplitude variation due to only the convergence of rays and the  $V_A$  decrease (without dissipation in the discontinuity). The dashed lines denote the jump  $U_{sh}$  of the plasma velocity component  $u$  in the shock wave, the solid ones – that of the plasma velocity magnitude. The horizontal axis is shown in the normalised time units, the vertical axis is shown in the units of the initial amplitude.

waves) through an inhomogeneous medium. To familiarise the readers with details of the method used, we refer them to the papers by Afanasyev and Uralov (2011) and Uralova and Uralov (1994). Besides, in Appendix A we give the set of nonlinear ray equations (see Equations (5)), which we solve to model the weak shock wave propagation, and in Appendix B we present derivation of the nonlinear ray equations.

Figure 5 shows the propagation of a weak shock wave in a cold plasma. Like the linear cold plasma case, the wave is captured by the null point and wraps around it. However, the propagation speed at the null point is non-zero owing to nonlinearity and the shock wave passes through the null point (cf. McLaughlin *et al.*, 2009) like a linear wave in a plasma with the small sound

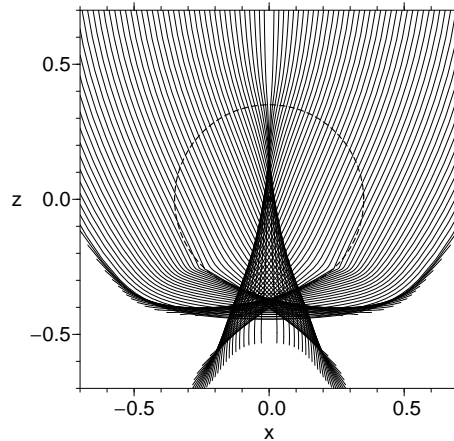


**Figure 7.** The propagation of a shock wave near a null point in a warm plasma. The dashed line denotes the location of the  $V_A = c$  layer, the solid ones are the rays. At the initial moment, the plane wave front was located at  $z_0 = 1$  and  $-1 \leq x \leq 1$ . The axes are shown in the normalised units.

speed. Therefore, in this case a caustic also arises in the small neighbourhood of the null point. This can be seen in Figure 5b, which shows the propagation pattern in a small area around the null point. The caustic is seen as the sharp border of a ray crowding. The amplitude of the wave tends to infinity at the caustic. This indicates again the places of significant plasma heating.

The wave front elements being close to the null point have higher amplitudes and therefore they travel faster. This results in forming a bulge in the wave front, which is visible in Figure 5b underneath the null point.

Figure 6 shows the shock wave amplitude. It decays considerably due to dissipation of the wave energy in the shock front. For comparison we also plot variation of the wave amplitude calculated with the assumption that there was no dissipation in the shock front. These plots demonstrate that a significant part of the shock wave energy is spent on plasma heating.

We have also considered the propagation of a weak shock wave in a warm plasma. In this case both nonlinearity of the wave and the non-zero sound speed in a plasma work in the same way. The shock wave propagates through the null point and a caustic is formed. The ray pattern is shown in Figure 7. The caustic is quite similar to that in Figure 3 for the linear warm plasma case, however it is shifted in the direction of the wave incidence. An effect of the non-zero sound speed appears to predominate over that of the wave nonlinearity. This is not unusual if we keep in mind that the nonlinear geometrical acoustics method should be applied only for weak shock waves. We also note that two caustic cusps are located at the  $V_A = c$  layer.

#### 4. Discussion and Conclusions

We have applied the nonlinear geometrical acoustics method to model the propagation of a fast-mode MHD wave near a 2D magnetic null point. We have considered both a linear wave and a weak shock and calculated their behaviour in cold and warm plasmas. We have also calculated the wave amplitude, using the ray approximation and the laws of solitary shock wave damping.

The nonlinear ray method allows one to trace the wave front and calculate the jumps of MHD quantities at the front only, but it does not give information on the downstream plasma flow evolution, since irreversible processes occur behind the shock front. In the propagation model used taking into account the refraction effect (*i.e.* the wrapping effect), the wave front can encounter plasma “upstream” that at an earlier time was described as “downstream”. In this sense, the presented nonlinear ray equations are valid for weak shock waves, if there are no subsequent shock front intersections. Nevertheless, to investigate plasma heating we calculate the caustic pattern, neglecting the modified downstream plasma, which is correct for weak shock waves. We note again that since subsequent evolution of the downstream plasma flow cannot be analysed with the method used, we do not discuss the transformation of a null point into a current sheet under the shock wave effect.

For a linear wave approaching the null point in a cold plasma, the analytical law of the amplitude growth has been found. The wave amplitude increases exponentially and therefore the initially linear wave transforms into a shock, which has encouraged us to investigate the case of shock wave propagation. This analytical law expressed by Equation (3) (and Equation (4)) is consistent with the analytical solution that was obtained for the problem of the incidence of a cylindrically symmetric fast-mode wave on a 2D null point (Syrovatskii, 1966; Craig and McClymont, 1991; Longcope and Priest, 2007). Indeed, in their solution the radial component of the plasma velocity in the wave grows as  $1/r$  with the distance  $r$  to the null point. In the cylindrically symmetric case all the rays are straight and directed to the null point. So we have the following ray equation:  $dr/dt = -V_A = -r$ , and hence we obtain:  $r \propto e^{-t}$ , *i.e.*, the wave amplitude grows exponentially, like that in Equation (3). The additional time dependence in Equation (3) is due to the plain (not cylindrical) initial wave front and represents the fact that all the rays are different and depend on initial coordinate  $x_0$ .

A complex caustic is formed around the magnetic null point. The wave amplitude tends to infinity at the caustic, resulting in plasma heating. The heating is distributed in space and occurs mainly out of the  $V_A = c$  layer if the initial wave front is rather extensive. However, the first heating associated with a central part of the wave occurs within the  $V_A = c$  layer. On the contrary, in the well-known case of a linear wave in a cold plasma, plasma heating takes place in a small vicinity of the null point. Since real null points in the solar corona appear to capture only a (central) part of the wave, while its outer part propagates away, the size of the  $V_A = c$  layer may be chosen as the spatial scale of plasma heating.

Nonlinearity of a wave is crucial for its propagation. A shock wave is able to pass through a null point even in a cold plasma. The growth of the shock

wave amplitude is restricted, since shock waves decay significantly due to the nonlinear energy dissipation in the shock front. Therefore along with the heating at a caustic, a substantial heating of plasma occurs in the neighbourhood of the null point. A significant part of the shock wave energy transforms into heat there.

Drawing the caustic pattern, we have explained the complicated surface of the wave front. A break of the wave front occurs at the caustic, thus triangles of the wave front arise when the front passes through a caustic cusp. The vertices of the triangles travel along the caustic lines.

To summarise we discuss a chance to estimate the magnitude of plasma heating associated with propagation of waves near a magnetic null point. Conversion of the wave energy into heat occurs due to dissipative processes in a plasma when the gradients of MHD quantities increase significantly. In a linear wave the gradients grow owing to the wave extent decrease as well as the amplitude growth as the wave approaches a null point. To estimate the value of the energy converted into heat in this case, one should consider non-ideal magnetohydrodynamics. In turn, in a shock wave the gradients of MHD quantities also originate at the wave front due to the nonlinear steepening of the wave profile. Here, the value of the energy converted is taken into account by the laws of shock wave damping. Since the sound speed in the real solar coronal plasma does not drop to zero, the wave extent can remain rather large, and so viscosity, thermal conductivity and finite plasma conductivity do not result in energy conversion. In such a case considerable plasma heating will occur due to the wave energy dissipation in the shock front, with the nonlinear heating predominating over heating at caustics. So, evaluating the difference between the shock wave amplitude and the amplitude calculated without dissipation in the discontinuity (as in Figure 6), one can provide some rough estimates about the plasma heating magnitude.

## Appendix

### A. Ray equations

The sets of ray equations have the following form in Cartesian coordinates:

$$\begin{aligned} \frac{dx}{dt} &= \left( a + N \frac{\kappa U_{sh}}{2} \right) \frac{k_x}{k} + k \frac{\partial a}{\partial k_x}, & \frac{dk_x}{dt} &= - \frac{\partial a}{\partial x} k, \\ \frac{dz}{dt} &= \left( a + N \frac{\kappa U_{sh}}{2} \right) \frac{k_z}{k} + k \frac{\partial a}{\partial k_z}, & \frac{dk_z}{dt} &= - \frac{\partial a}{\partial z} k, \end{aligned} \quad (5)$$

where  $k_x, k_z$  and  $k$  are the components of the wave front normal  $\mathbf{k}$  and its magnitude respectively, and  $N$  the numerical factor switching the linear and nonlinear regimes of the wave propagation. We should take  $N = 0$  for studying a linear wave and  $N = 1$  for a weak shock one.

The adjoint set consists of differential equations for the derivatives  $\partial x / \partial \eta$ ,  $\partial z / \partial \eta$ ,  $\partial k_x / \partial \eta$ ,  $\partial k_z / \partial \eta$  and is derived by differentiating Equations (5) (with

$N = 0$ ) with respect to the ray coordinate  $\eta$ :

$$\begin{aligned}
 \frac{d}{dt} \left( \frac{\partial x}{\partial \eta} \right) &= \frac{k_x}{k} \frac{\partial a}{\partial \eta} + \frac{a}{k} \frac{\partial k_x}{\partial \eta} - \frac{ak_x}{k^2} \frac{\partial k}{\partial \eta} + \frac{\partial a}{\partial k_x} \frac{\partial k}{\partial \eta} + k \frac{\partial}{\partial \eta} \left( \frac{\partial a}{\partial k_x} \right), \\
 \frac{d}{dt} \left( \frac{\partial z}{\partial \eta} \right) &= \frac{k_z}{k} \frac{\partial a}{\partial \eta} + \frac{a}{k} \frac{\partial k_z}{\partial \eta} - \frac{ak_z}{k^2} \frac{\partial k}{\partial \eta} + \frac{\partial a}{\partial k_z} \frac{\partial k}{\partial \eta} + k \frac{\partial}{\partial \eta} \left( \frac{\partial a}{\partial k_z} \right), \\
 \frac{d}{dt} \left( \frac{\partial k_x}{\partial \eta} \right) &= -\frac{\partial k}{\partial \eta} \frac{\partial a}{\partial x} - k \frac{\partial}{\partial \eta} \left( \frac{\partial a}{\partial x} \right), \\
 \frac{d}{dt} \left( \frac{\partial k_z}{\partial \eta} \right) &= -\frac{\partial k}{\partial \eta} \frac{\partial a}{\partial z} - k \frac{\partial}{\partial \eta} \left( \frac{\partial a}{\partial z} \right),
 \end{aligned} \tag{6}$$

where

$$\begin{aligned}
 \frac{\partial a}{\partial \eta} &= \sum_{\alpha} \left( \frac{\partial a}{\partial r_{\alpha}} \frac{\partial r_{\alpha}}{\partial \eta} + \frac{\partial a}{\partial k_{\alpha}} \frac{\partial k_{\alpha}}{\partial \eta} \right), \quad \frac{\partial k}{\partial \eta} = \frac{1}{k} \sum_{\alpha} k_{\alpha} \frac{\partial k_{\alpha}}{\partial \eta}, \\
 \frac{\partial}{\partial \eta} \left( \frac{\partial a}{\partial k_{\beta}} \right) &= \sum_{\alpha} \left( \frac{\partial}{\partial r_{\alpha}} \left( \frac{\partial a}{\partial k_{\beta}} \right) \frac{\partial r_{\alpha}}{\partial \eta} + \frac{\partial}{\partial k_{\alpha}} \left( \frac{\partial a}{\partial k_{\beta}} \right) \frac{\partial k_{\alpha}}{\partial \eta} \right), \\
 \frac{\partial}{\partial \eta} \left( \frac{\partial a}{\partial r_{\beta}} \right) &= \sum_{\alpha} \left( \frac{\partial}{\partial r_{\alpha}} \left( \frac{\partial a}{\partial r_{\beta}} \right) \frac{\partial r_{\alpha}}{\partial \eta} + \frac{\partial}{\partial k_{\alpha}} \left( \frac{\partial a}{\partial r_{\beta}} \right) \frac{\partial k_{\alpha}}{\partial \eta} \right), \\
 r_{\alpha} &= x, z; \quad k_{\alpha} = k_x, k_z.
 \end{aligned}$$

The numerical coefficient  $\kappa$  depends on the plasma beta as well as the angle  $\alpha$  between the wave front normal and the magnetic field as

$$\kappa = \frac{(1 + \beta + Q_1)(\beta(\gamma - 2) + 3Q_1) - 2\beta \cos^2 \alpha (\gamma - 1 - \beta + Q_1)}{2Q_1(1 + \beta + Q_1)},$$

where  $Q_1 = \sqrt{(1 + \beta)^2 - 4\beta \cos^2 \alpha}$ ,  $\beta = c^2/V_A^2$ , and  $\gamma = 5/3$  is the adiabatic index. Values of  $\kappa$  are restricted by the limits  $1/2 \leq \kappa \leq 3/2$  and are shown in Figure 8. When the wave crosses the  $V_A = c$  layer along the magnetic field ( $\alpha = 0$ ),  $\kappa$  has a jump.

Set of ray equations (5) is not closed in the nonlinear case since it includes the wave amplitude  $U_{sh}$ . It can be calculated with the laws of solitary shock wave damping (Uralov, 1982), which are derived by using values of the amplitude and duration of a simple wave from which the shock forms:

$$U_{sh} = u_1 \left( 1 + \frac{\tau_1}{T_0} \right)^{-1/2}, \quad \frac{d\tau_1}{dt} = \frac{\kappa u_1}{a}, \tag{7}$$

where  $\tau_1$  is the duration increment of the simple wave with amplitude  $u_1$ ;  $T_0$  is the initial duration of the shock wave. The value of  $u_1$  can be found from an equation similar to Equation (2).

Solving sets of ordinary differential equations (5), (6) and (7) numerically we are able to model the propagation of fast-mode MHD waves.

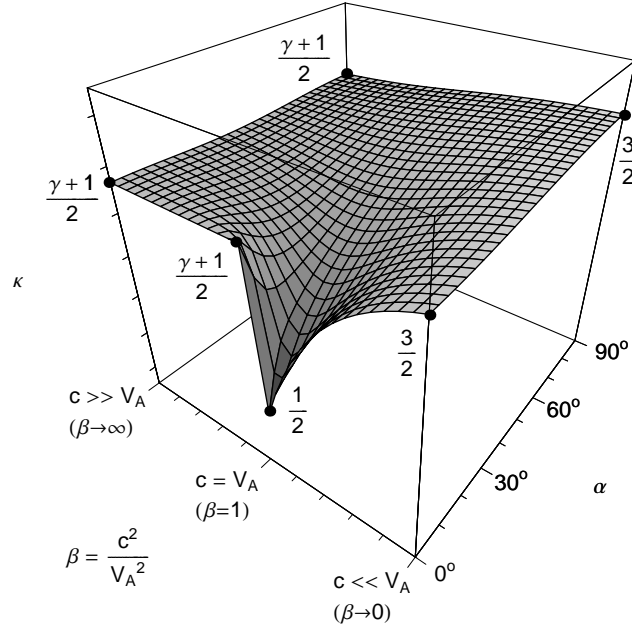


**Figure 8.** The values of coefficient  $\kappa$ . The points at the surface denote the relevant values corresponding to some particular cases of propagation. There is a jump of  $\kappa$  at  $\alpha = 0$  and  $\beta = 1$ .

## B. Derivation of nonlinear ray equations

The sets of ray equations can be obtained with a different method which does not use the eikonal expansion of the MHD equations. In fact, this method is different only in form and it is more convenient for analysing nonharmonic waves which we deal with in this paper. We apply this method for deriving the set of nonlinear ray equations.

The moving surface of the wave front can be described by the equation  $\Phi(\mathbf{r}, t) = 0$ , or in the differential form  $d\Phi = 0$ . Let a small surface element displace by  $d\mathbf{r}$  in time  $dt$ . Then we have:

$$\frac{\partial \Phi}{\partial t} + \left( \text{grad} \Phi \cdot \frac{d\mathbf{r}}{dt} \right) = 0, \quad (8)$$

where  $d\mathbf{r}/dt = \mathbf{q}$  is the velocity of the front element and  $\text{grad} \Phi$  the wave front normal by definition. The scalar product can be rewritten as  $q_n |\text{grad} \Phi|$ , with the  $q_n$  denoting the normal speed of the wave front. So we obtain a partial differential equation.

If we consider a linear fast-mode MHD wave,  $q_n = a$ , and we have the same “eikonal” equation and the same set of ray equations as presented in Section 2.1 and Appendix A (the case of  $N = 0$ ), respectively. However, we are interested in the weak shock wave propagation. The normal speed of the weak shock front can be derived from the jump conditions across a MHD discontinuity, and it is

equal to  $a + \kappa U_{sh}/2$  in the nonlinear acoustics approximation. Substituting it into Equation (8) and solving with the method of characteristics, we obtain the set of ray equations, which is similar to the linear one and in which substitution  $a \rightarrow a + \kappa U_{sh}/2$  has been performed. In these new ray equations the additional terms  $\partial U_{sh}/\partial k_\alpha$  and  $\partial U_{sh}/\partial r_\alpha$  appear. We neglect them, keeping only quantity  $U_{sh}$  itself and omitting its derivatives, exploiting the nonlinear geometrical acoustics approximation. Thus we obtain the set of nonlinear ray equations (5) (with  $N = 1$ ) presented in Appendix A.

**Acknowledgements** We thank the anonymous referee for helpful comments and valuable suggestions. We also thank the editors for careful reading of the manuscript and useful comments. A.A. is very grateful to the scientific organising committee of the ESPM-13 for financial support.

The research was supported by the Russian Foundation of Basic Research (Grant No. 12-02-00037) and a Marie Curie International Research Staff Exchange Scheme Fellowship within the 7th European Community Framework Programme as well as Siberian Branch of the Russian Academy of Sciences (Lavrentyev Grant 2010–2011). It was also supported by the Ministry of Education and Science of the Russian Federation (State Contracts 16.518.11.7065 and 02.740.11.0576).

## References

- Afanasyev, A.N., Uralov, A.M.: 2011, *Solar Phys.* **273**, 479.
- Blokhintsev, D.I.: 1981, *Acoustics of an Inhomogeneous Moving Medium*, 2nd edn., Nauka, Moscow (in Russian).
- Craig, I.J.D., McClymont, A.N.: 1991, *Astrophys. J. Lett.* **371**, L41.
- Foullon, C., Verwichte, E., Nakariakov, V.M., Fletcher, L.: 2005, *Astron. Astrophys.* **440**, L59.
- Gruszecki, M., Vasheghani Farahani, S., Nakariakov, V.M., Arber, T.D.: 2011, *Astron. Astrophys.* **531**, A63.
- Kravtsov, Y.A., Orlov, Y.I.: 1990, *Geometrical Optics of Inhomogeneous Media*, Springer-Verlag, Berlin.
- Kulikovskiy, A.G., Lyubimov, G.A.: 2005, *Magnetic Hydrodynamics*, 2nd edn., Logos, Moscow (in Russian).
- Longcope, D.W.: 2005, *Living Reviews in Solar Physics* **2**, 7.
- Longcope, D.W., Priest, E.R.: 2007, *Phys. Plasmas* **14**, 122905.
- McLaughlin, J.A., Hood, A.W.: 2004, *Astron. Astrophys.* **420**, 1129.
- McLaughlin, J.A., Hood, A.W.: 2006a, *Astron. Astrophys.* **452**, 603.
- McLaughlin, J.A., Hood, A.W.: 2006b, *Astron. Astrophys.* **459**, 641.
- McLaughlin, J.A., Ferguson, J.S.L., Hood, A.W.: 2008, *Solar Phys.* **251**, 563.
- McLaughlin, J.A., Hood, A.W., De Moortel, I.: 2011, *Space Sci. Rev.* **158**, 205.
- McLaughlin, J.A., De Moortel, I., Hood, A.W., Brady, C.S.: 2009, *Astron. Astrophys.* **493**, 227.
- Nakariakov, V.M., Foullon, C., Verwichte, E., Young, N.P.: 2006, *Astron. Astrophys.* **452**, 343.
- Parnell, C.E., Smith, J.M., Neukirch, T., Priest, E.R.: 1996, *Phys. Plasmas* **3**, 759.
- Syrovatskii, S.I.: 1966, *Soviet Journal of Experimental and Theoretical Physics* **23**, 755.
- Uralov, A.M.: 1982, *Magnitnaya Gidrodinamika* No. 1, 45 (in Russian).
- Uralova, S.V., Uralov, A.M.: 1994, *Solar Phys.* **152**, 457.



